

RESEARCH PAPER

Utilizing the Characteristics of Graphene Nano-Platelets to Improve the Cross-Linking Density of a Rubber Nano-Composite

Hasan Shakir Majdi¹, Laith Jaafer Habeeb²

¹ Al-Mustaqbal University College, Babylon – Hillah

² University of Technology / Training and Workshop Center, Baghdad – Iraq

ARTICLE INFO

Article History:

Received 08 May 2020

Accepted 28 July 2020

Published 01 December 2020

Keywords:

Graphene Nanoplatelets

NBR Rubber

Rubber nanocomposites

ABSTRACT

Graphene nanoplatelets (GNP) / Acrylonitrile butadiene rubber (NBR) nanocomposites were prepared by solutions mixing method and vulcanized effectively. GNP suspension dispersed homogeneously in a well-suited solution of NBR up to 2.4 phr and characterized by X-ray Diffraction (XRD). The influence of GNP on the cross-linking of GNP/NBR nanocomposites structure has been characterized and studied by the cure characteristics and swelling tests. The results showed that the cross-linking density was enhanced to 42.3% compared to that of unfilled NBR by reducing the swelling ratio to 19.7% at 1.2 phr of the GNP. Thus, the mechanical properties were investigated and revealed that the modulus at 100% elongation (M_{100}) improved to about 155% and the hardness to about 13%. Those results were verified via the morphology analyzing using Scanning Electron Microscopy (SEM) and the enhancement of the storage modulus as a function of temperature in the rubber nanocomposite to about 100% utilizing Dynamic Mechanical Analysis (DMA) at the same content 1.2 phr of GNP.

How to cite this article

Shakir Majdi H., Jaafer Habeeb L. Utilizing the Characteristics of Graphene Nano-Platelets to Improve the Cross-Linking Density of a Rubber Nano-Composite. J Nanostruct, 2020; 10(4): 723-735. DOI: 10.22052/JNS.2020.04.005

INTRODUCTION

GNP is a type of graphitic nano fillers, consisting of stacked two dimensional (2D) graphene sheets, having exceptional physical properties. It is considered as an ideal carbonic nanofiller and strengthening constituent to improve the properties of a wide variety of polymers. Also, the high surface area makes the GNP as a distinct filler, showing the advantages in the improvement of the interfacial adhesion with the most polymeric matrices, if compared with other carbonic nano fillers [1].

The stacked layers of GNP are combined with each other via feeble forces of Van Der Waals with an interlayer distance of about 0.35 nm [2]. Those layers having thickness differs about several

nanometers lead to an increased specific surface area more than 2000 m²/g [3]. Moreover, GNP dimensions are affected by certain treatments, such as oxidization, heating and ultra-sonication [4]. In addition, GNP has proven their importance as vigorous, adaptable and economical fillers in the composite materials at fewer contents [1, 5]. As incorporating nanofiller in a polymeric matrix, the desired characteristics with high physical properties of the GNP can be transferred to the polymeric nanocomposites [3-7]. Therefore, there is a significant development of elastomer composites showing through the mechanical performance, thermal stability, gas barrier property and other attributes [8-11].

There has been a lot of research demonstrating that the direct melt blending is not sufficient



This work is licensed under the Creative Commons Attribution 4.0 International License.

To view a copy of this license, visit <http://creativecommons.org/licenses/by/4.0/>.

for the considerable dispersion quality and high properties of GNP/elastomer nanocomposites. Several modified solution-mixing methods have been improved, which indicated a significant development when comparing with direct mixing [11-14]. Overall, the main concern in the fabrication of GNP/elastomer nanocomposites is the homogeneous dispersion of GNP in the matrix of rubber [15].

It is found that all the carbonic nano fillers showed great physical properties in the carbon/polymer composites, the effect on the processing is noticeable. Some research [1, 7] reported that the carbon black (CB) and carbon nanotubes (CNTs) have the highest viscosity in different ranges of the filler contents compared with the GNP filled polymer nanocomposites which indicate better process ability for GNP. This is associated with the capability of different nano fillers in numerous polymers to create network structures that could constrain the mobility of the polymeric chains [16-18].

When a polymer is placed in an active solvent, it absorbs a percentage of the solvent, which makes it swell. The extent of the elastomer's size represents the converse between two forces, swelling deformation and elastic force, which are generated by the polymer chains. The volumetric swelling attains the steady state when the forces are at equilibrium with each other. Furthermore, the molecular weight between the crosslinks can be computed by the Flory interaction parameter of the polymer and solvent system [19-21].

In the other side, vulcanization is an essential treatment in the rubber fabrication, which is creating and increasing the elastomeric chain crosslinking. The fillers addition causes the change in the torque values and the curing times. In addition, the fillers dispersion in the rubber composites can be clarified employing the minimum torque (M_L) and maximum torque (M_H) which are measured during the curing. M_H corresponds to the high surface area of the fillers that create vigorous interfacial adhesion with the matrix and, in turn, gives an influential content transfer between the rubber matrix and the filler [17, 21]. The change in the torques with the filler contents is a measure of the filler-rubber adhesion and enhancement of cross-linking density [22].

The improvement of GNP/Polymers nanocomposites characteristics has been a passionate research subject in last decade.

The superior mechanical properties of the nanocomposites prepared were attributed to the strong interface bonding due to that the high dispersion quality of GNP can benefit the load transfer within the elastomeric composites. Therefore, the improvement in the rubber composite elastic modulus and tensile strength are expected with addition of GNP [23-26].

This study aims to disperse GNP into NBR using solution-mixing method to prepare a homogenous GNP/NBR rubber nanocomposite with low agglomeration of GNP. Due to the excellent link of NBR molecules with many types of fillers via the free-radical initiators, the structure could be enhanced by transferring the GNP desirable characteristics to NBR properties. Characterization of various contents of GNP in GNP/NBR rubber nanocomposites verified the homogeneity and interfacial adhesion of the GNP with NBR molecular chains. Furthermore, cross-linking density and sorts of mechanical tests have confirmed the improvement in the rubber nanocomposite structure.

MATERIALS AND METHODS

Acrylonitrile butadiene rubber (Krynac 3345f) was obtained from Malaysia Rubber Company having the following specifications: Mooney viscosity ML (1+4), 100°C. Graphene nanoplatelets (GNP) (20 nm thickness) were purchased from XG Sciences Inc. Dimethyl methyl formamide (DMF), Acetone, Toluene and Polyoxyethylene octyl phenyl ether – (Triton X-100) were purchased from R & M Chemical Marketing. Other additives of the vulcanization, such as Zinc oxide, Sulfur, Steric Acid, N-Cyclohexyl-2-benzothiazole sulfonamide (CBS) as an accelerator and N-Isopropyl-N-phenyl-P-phenylenediamine 4010NA (IPPD) as an oxidant agent, were purchased from RC Chemical Co. Ltd.

GNP/NBR rubber nanocomposite preparation

Preparation of NBR and GNP solutions

Selecting a proper solvent for dissolving the Acrylo-NBR, and the compatibility of GNP suspension solution with this matrix to prepare (GNP/NBR) rubber nanocomposite have been optimized experimentally. The NBR was firstly cut into small fragments, and then three samples of 3g of NBR were dissolved in three beakers of 100 mL containing three solvents, which were: acetone, toluene, and DMF. A magnetic stirrer mixer was used with 200 RPM for dissolving the



Fig. 1. Steps of preparation vulcanized (GNP/NBR) rubber nanocomposite

Table 1. formulation of (GNP/NBR) rubber nanocomposites and vulcanization additives

GNP/NBR nanocomposites		Vulcanization formulation	
Composites	phr	Agents	phr
NBR	0.0	Zinc Oxide	4.0
GNP/NBR1	0.2	Steric Acid	1.5
GNP/NBR2	0.6	Sulfur	2.0
GNP/NBR3	1.2	CBS (Accelerator)	0.5
GNP/NBR4	2.4	IPPD (Anti-Oxidant)	1.0

NBR totally at 65°C. The analysis of viscosity was conducted via using a viscometer (Brookfield) according to ISO 2555. Subsequently, the viscosity and dissolution times were measured, and the qualitative observation has corresponded. The compatibility of the GNP suspension with the NBR solution was verified by exfoliating of 5 mg of GNP with a 0.3 g/cm³ density in 20 mL of distilled water, 1.8% TritonX-100/H₂O using a probe-sonicator (Sonics-VCX750) for 60 minute.

Dispersion of GNP into the NBR nanocomposite

GNP/NBR rubber nanocomposites were prepared by following the physical and chemical approaches, as shown in Fig. 1.

Mechanical mixing with a gradual speed of 500-1200 rpm was performed by pouring different contents of GNP (0.2, 0.6, 1.2, and 2.4) phr in 40 g of dissolved NBR. After 1 hour, the rubber nanocomposite mixtures started to coagulate, and the final mixture of the GNP/NBR rubber nanocomposite was qualitatively observed. The rubber nanocomposite blend was dried inside a vacuum oven at 70°C under 0.08 MPa pressure until the weight was unchanged. Then, a two-roll mill was used to add and mix the vulcanization

materials based on the standard formula, as shown in Table 1. Zinc oxide and stearic acid were added to the mixture for 15-20 minute, followed by adding sulfur, antioxidant and the CBS accelerator. About 10 g of each sample was inserted into the rheometer cavity under high pressure and elevated temperature to determine the torque, temperature and time before molding. A die was used for molding 30 g of rubber nanocomposite. Consequently, a hot plates press type (Lab Tech Eng. Co. Ltd) machine was used to mold the sheets of vulcanized GNP/NBR rubber nanocomposites according to (ASTM D3182). The heating temperature was 160°C, and the hydraulic compression was 10 MPa.

Characterization of the GNP/NBR Nanocomposites

The cure characteristics tests were performed using Rheometer MDR-2000 type (Monsanto), where the conical disc of the rheometer was oscillated with a small angle which exerted a shear strain on the test sample. The tests were performed according to ISO 289-2 [27-29]. The torque required to rotate the disc was measured as a function of the scorch time (Ts₂) and time to 90% cure T₉₀. The cure time is equal to the time to

reach x% of the torque increase (T_x), [30] i.e.:

$$T_x = M_L + x / 100 (M_H - M_L) \quad (1)$$

The morphology of the surfaces of the unfilled vulcanized NBR sample and vulcanized GNP/NBR rubber nanocomposites samples were characterized by SEM (Hitachi-S3400N). It is worth to mention that after tensile tests performed, the fractured samples of the tensile tests were coated with a thin film of gold using a vacuum sputtering technique to become response to the scanning and imaging the surfaces features. Then, the structure was observed by several SEM micrographs viewed at various magnification levels (100x-2000x).

The GNP dispersion level in the matrix of NBR and the intercalated structures crystallinity were characterized via using the X-ray Diffraction device (Shimadzu 6000) having the monochromatic Cu K- α radiation and $\lambda = 0.154$ nm. The other conditions were continuous scanning with a drive axis q to $2q$, a range of scan (2.000-40.000) and a speed of scan (2.000 deg./min).

Characterization of the crosslinking density using swelling test was performed for the samples of the unfilled (NBR) and (GNP/NBR) rubber nanocomposites having different contents of GNP. Experimentally, the test was achieved by equilibrating the samples in the toluene at ambient temperature. The swelling ratio (Q_r) could be calculated by [31]:

$$Q_r = (W_{sw} - W_i) / W_{dr} \quad (2)$$

Where, W_{sw} is the weight of the sample after swelling (48 hour immersion in toluene), W_i is the initial weight before the test, and W_{dr} is the weight after drying at 70°C (until no further change occurred in the weight).

The mechanical characteristics of the NBR and GNP/NBR rubber nanocomposite structures were investigated through the tensile strength test. The tensile machine (Instron-5566) with 10 KN was used according to ISO37. The dog bone type of samples according to (ASTM D412) had approximate dimensions of (25×4×2) mm. The strain rate (rate of stretching) for all the tests was 500 mm/min for three samples of each content of GNP. The influence and efficiency of GNP in GNP/NBR nanocomposite were observed via the tensile stress and strain, elongation and modulus from the yield points to the breakpoints.

Hardness property was another mechanical strength measurement which was performed by

(Shore D) tester for the unfilled NBR and GNP/NBR nanocomposite samples. The thickness of the sample was 8 mm, and the applied force was the weight of 200 g according to (ASTM D2240-05).

Dynamic mechanical analysis (DMA) test was used for measuring the storage modulus (E') and the loss modulus (E'') to find the dynamic loss factor ($\tan\delta$), which is called the ratio of energy losing of NBR before and after reinforcement by GNP. The used instrument was DMA Q800 V20.24, temperature range was from (-60) to (60°C) under nitrogen atmosphere at a heating rate 3°C/min from (-50) to (50°C).

All the characterization data and results were observed and tabulated for the analyzing procedures, as shown in section 2.4.

RESULTS AND DISCUSSION

Cure characteristics

The torque-time curves in Fig. 2 showed the cure characteristics of NBR and GNP/NBR nanocomposite with different contents of GNP at $T=160^\circ\text{C}$. Generally, the minimum torque (M_L) of all samples in the rheometer was tending to decrease initially during the short time of scorch time (T_s) due to the softening of the rubber before the thermal curing. Subsequently, the torque increases up to the maximum (M_H) during the first 5 minutes due to the crosslinks formation of the rubber chains for all the samples. This is due to the interaction of the vulcanization additives with the initiators of NBR rubber chains. The torque values then reached the plateau, which indicates the completion of the curing at T_{90} (time taken for obtaining 90% of the curing).

When the filler disperses in several polymers, it can form a network, which can constrain the mobility of the polymeric chains [32]. Adding 0.2 to 1.2 phr of GNP in GNP/NBR nanocomposites showed an increase in the values of M_H and torque at 90% of the curing (M_{90}), as shown in Table 2 and Fig. 3-a. The enhancement in the values of the torque is usually related to the rubber chains crosslinking degree, which increases the crosslinking density of the composite. Thus, it is contributed to the stiffness of the rubber nanocomposite. However, the low increase in the torque values at low contents were attributed to the low viscosity of the mixture. This might be due to the lubricant property of the graphene derivatives [21, 33].

In addition and according to Hernandez et al.

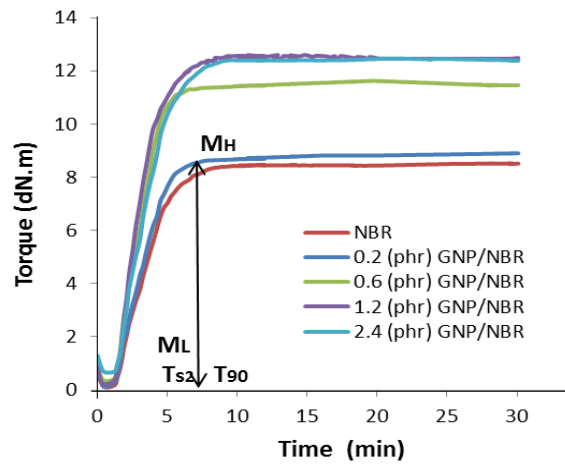


Fig. 2. Effect of GNP contents on the torque-time behavior of NBR at T=160°C.

Table 2. NBR and GNP/NBR rubber nanocomposites curing data and results

Composite	GNP (phr)	M _H (dN.m)	M _L (dN.m)	M ₉₀ (dN.m)	T _{S2} (min)	T ₉₀ (min)	CRI at T ₉₀
NBR	0.0	11.39	0.51	10.30	1.47	5.97	22.22
GNP/NBR1	0.2	11.46	0.42	10.35	1.37	5.72	22.99
GNP/NBR2	0.6	12.85	0.43	11.60	1.44	5.41	25.19
GNP/NBR3	1.2	12.44	0.48	11.24	1.61	3.74	46.95
GNP/NBR4	2.4	11.56	0.50	10.45	1.83	4.36	40.53

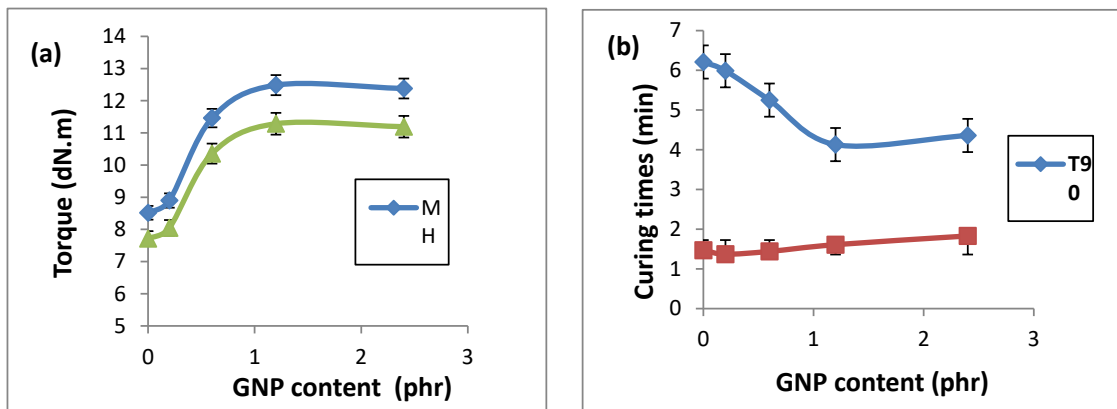


Fig. 3. The effect of GNP contents on the (a) torques, (b) times of initial and 90% of curing.

[34], the carbon-based fillers addition can delay the vulcanization onset. The other essential parameter of the curing curve is the curing time. As shown in Fig. 3-b, there was no increase in the scorch time (Ts2) at low content of GNP, and

a slight increase at 1.2 and 2.4 phr of GNP was appeared. This indicates to the free mobility of the rubber molecules chains due to the low viscosity, which is relative ease of the GNP/NBR rubber nanocomposite process ability. While, the curing

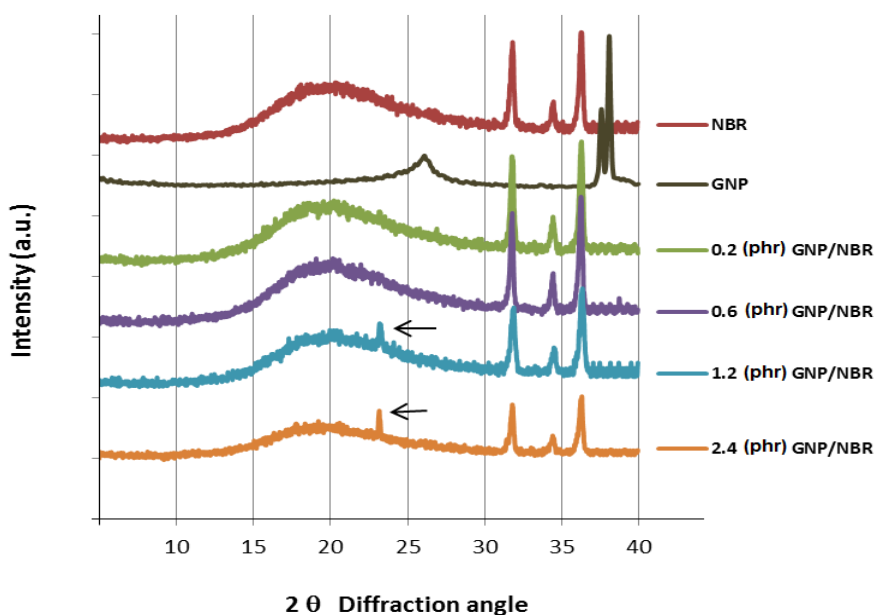


Fig. 4. The XRD (diffraction patterns) of GNP, NBR and GNP/NBR nanocomposites for various contents.

time was reached T_{90} in the vulcanized unfilled NBR at 5.97 min and then was noted to be reducing with raising GNP contents to about 4.36 min. This is demonstrated a homogeneous filler dispersion within the matrix of rubber and could promote an increment in the product formation rate. Furthermore, adding GNP led to the increase in the rate of the curing reaction, which contributed to the increase of the cure rate index (CRI), as shown in Table 2. It is expressed by $100/(T_{90} - T_{s2})$, this could be credited to the ability of filler for accelerating the vulcanization reaction. The cure characteristics of GNP/NBR nanocomposit were approved in this test via the torque increment due to the increase in the crosslinking density which has a profound influence on the mechanical strength as discussed in the later part of this work.

The XRD test

The homogeneous GNP distribution in the matrix of (NBR) was more corroborated via the analysis of XRD. As it can be noticed in Fig. 4, the (GNP) diffraction peak emerged at $2\theta = 26.65^\circ$. The interlayer d-spacing between the (GNP) layers was calculated using Bragg's equation (3);

$$n\lambda = 2d \sin \theta \quad (3)$$

It was 0.34 nm of distance and consistent

with the layer spacing of graphite, where n is the diffraction order and λ is the wavelength. The unfilled NBR characteristic wide peak obtained at $2\theta = 19^\circ$ and had a slight shift when NBR filled with different GNP contents. This might indicate that the GNP was dispersed entirely and suggest an intense intercalation between GNP and NBR. Nevertheless, the rubber nanocomposites (XRD) pattern with low contents of GNP (0.3 and 0.6 phr) showed the peaks of diffraction same to that of the unfilled NBR. That explains that GNP were totally exfoliated into the monolayer or few layers, and dispersed homogenously into the NBR matrix as approved in other research [35, 36]. The GNP formed crystalline networks in the rubber matrix, which enhanced the composites mechanical properties, as depicted in the results of tensile test. Nonetheless, GNP was no single graphene layers but rather consisted of a number of stacked plates of graphene [36]. Therefore, a few agglomerations of the GNP might be reproduced in the rubber composites at the content of 1.2 and 2.4 phr of the GNP, which appeared as a small peak at $2\theta = 23.5^\circ$. This result agrees well with the conclusion in the curing characteristics tests. GNP dispersion in a polar elastomer like NBR exhibits an excellent physical intercalation depending on the processing techniques and affinity between

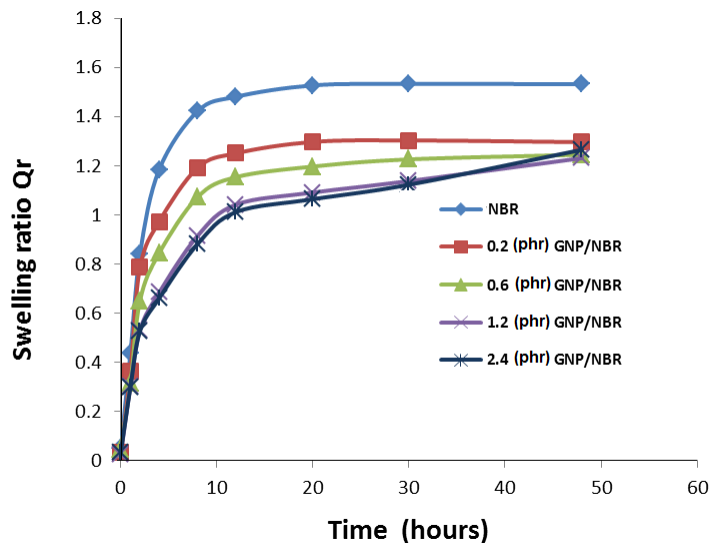


Fig. 5. Swelling ratio, in toluene for 48 hours, as a function of the time of unfilled NBR and (GNP/NBR) nanocomposites with various contents of GNP.

Table 3. Swelling test parameters and crosslinking density (n) of (GNP/NBR) nanocomposites rubber.

GNP (phr)	W _i (g)	W _{sw} (g) 48h	W _{dr} (g)	Q _r ratio	Q _r /Q ₀ Relative	(n) x 10 ⁻³ (mol/cm ³)
0.0	0.332	0.844	0.334	1.533	1.000	9.457
0.2	0.334	0.768	0.335	1.296	0.845	12.289
0.6	0.357	0.804	0.359	1.245	0.812	13.182
1.2	0.323	0.722	0.324	1.231	0.803	13.455
2.4	0.335	0.761	0.336	1.265	0.825	12.812

the platelets. Any improvement in the crystallinity degree of the composite is due to the good dispersion of GNP, which can also play a major role in enhancing the physical properties of the GNP/NBR nanocomposite, as noted in the mechanical properties next section.

Crosslinking density

Most rubbers are sensitive to the solvents in various degrees. Therefore, swelling rate in the rubber composites is dependent on the type of solvent, rubber polarity, type of filler and its content. It can be seen in Fig. 5 that the unfilled vulcanized NBR sample showed a rapid swelling rate and a high swelling ratio (Q_r) at the first hours, but the vulcanized (GNP/NBR) rubber nanocomposites exhibited less increase in Q_r with the same time. According to the standard of the swelling test, the rate became stable at the final

equilibrium after 48 h [15, 19]. The saturation limit of solvent absorption might be attributed to the degree of the crosslinking of the NBR chains which is explained in term of density.

In addition, it's called the density of crosslink (n), which is computed by using the equation of Flory–Rehner, and the formula became as below:

$$n = V_m \cdot \frac{[v_2^{1/3} - v_2/2]}{-[\ln(1-v_2) + v_2 + Xv_2^2]} \tag{4}$$

Where, v₂ is the volume fraction given by (v₂=1/Q_r), V_m is the molar volume of toluene, which is equal to (106.3 mL/mole), and X is equal to 0.35. [19-21].

Table 3 demonstrates the parameters of the swelling test.

The results showed that Q_r of the solvent that has been absorbed by the NBR to the



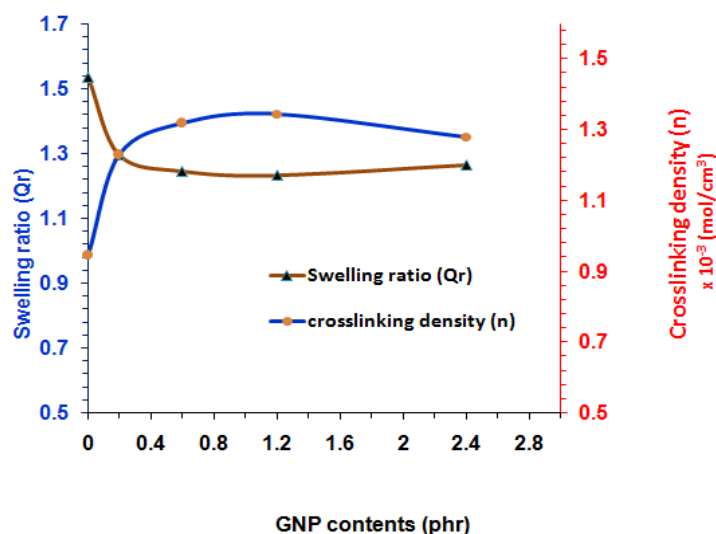


Fig. 6. Swelling ratio of GNP/NBR rubber nanocomposite and the crosslinking density.

original weight was reduced as the GNP contents increased, as shown in Fig. 6. The decrease in (Q_r) was continuing slightly via the increment in the contents of GNP in the nanocomposite until reaching 2.4 phr of GNP, which represent the decline stage. Where, at 2.4 phr, there was no improvement in the crosslinking and it is started to form some defects which reduces the swelling resistance.

Thus, swelling ratio decreased to about 19.7% at 1.2 phr of GNP. Furthermore, in the same figure, GNP had improved the crosslinking density to 2.3% at the same content of 1.2 phr of GNP due to the high physical intercalation between the GNP and the NBR matrix. The effective rubber nanocomposite curing was agreed with the improvement in the crosslinking density results. The increment in the network density of the NBR nanocomposite chains was responsible for the enhanced mechanical strength.

Mechanical strength

There are certain factors have an influence on the mechanical performance of the rubber composites, such as the compatibility of the filler, method of the filler dispersion, and composites preparation. The differences in the stress-strain behavior of the NBR rubber and GNP filled NBR based on the GNP content are shown in Fig. 7. Adding GNP to the NBR showed a noticeable increase in the tensile strength. At the maximum

content of 1.2 phr GNP, the tensile stress was increased by 42%, and the elongation at break was decreased by 8.3%. The intrinsic properties of GNP, structure and the physical interaction with the host matrix NBR improved the structure linking. The role of GNP is the enhancement of the interface and the load transfer between GNP and NBR which led to improve the tensile strength as investigated with other polymers [37,38]. However, the increment of GNP up to 2.4 phr in the NBR composite had no significant effect on the tensile parameters of the rubber nanocomposite (over threshold percolation). Also, the modulus of the GNP/NBR rubber nanocomposite improved when the contents of GNP increased.

As shown in Fig. 8, at 1.2 phr GNP, the modulus of the composite at 100% elongation (M_{100}) was increased by 155%. It is worth mentioning that increasing the content of the GNP in the GNP/NBR composites reduced the elastomer chains mobility that resulted in the reduction in the elongation, as shown in the Fig. 8.

However, the increment in the extension at break may be attributed to the sliding of GNP, which could be taken as a plasticizer effect. As reported, GNP is effective comparing to the natural graphite due to the superior dispersion ability, high surface adhesion and stronger interface linking [39, 40-44].

The resistance of GNP/NBR rubber nanocomposites surfaces against the external concentrated

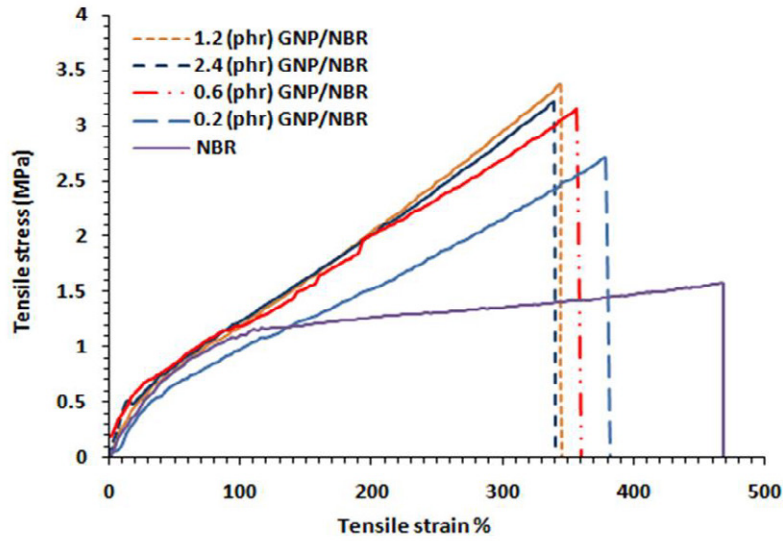


Fig. 7. The stress-strain curves of (NBR) and (GNP/NBR) rubber nanocomposites.

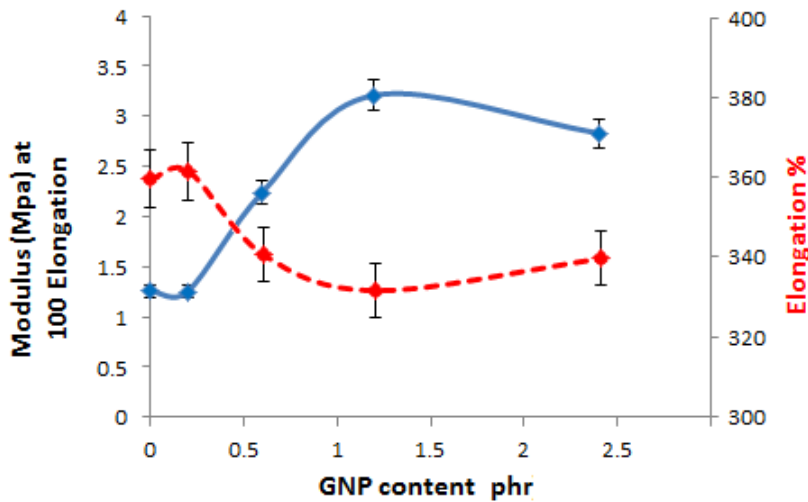


Fig. 8. Modulus and Elongation% of NBR and GNP/NBR rubber nanocomposites at different contents of GNP

stresses was improved due to GNP existence. Thus, there was an increment in the value of the hardness as the content of GNP increased in the rubber composite and reached the maximum at 1.2 phr of GNP. The hardness of the GNP/NBR rubber nanocomposite was increased about 13% more than the unfilled NBR, as shown in Table 4. The thermal curing of the rubber composites sheets by hot press molding might enhance the crosslinking density of GNP with the NBR molecular chains and improved the surface density and hardness.

Morphology of the GNP/NBR rubber nanocomposite

The morphology of vulcanized unfilled NBR and the level of GNP dispersion into the GNP/NBR rubber nanocomposite were investigated. The SEM micrograph imaging of the cross section of surface for two fractured tensile test samples was performed. The first sample of the vulcanized unfilled NBR displayed in Fig. (9-a) at 100x magnification shows the nature of surfaces due to the fracture stress and the distribution of the

Table 4. Hardness of (GNP/NBR) nanocomposite rubber using Shore D, sample's thickness = 8 mm, according to STAM D416.

Rubber and Composite	GNP content (phr)	Density (g/cm ³)	Hardness Shore D
NBR	0.0	1.00	10.5
GNP/NBR	1.2	1.04	12.1

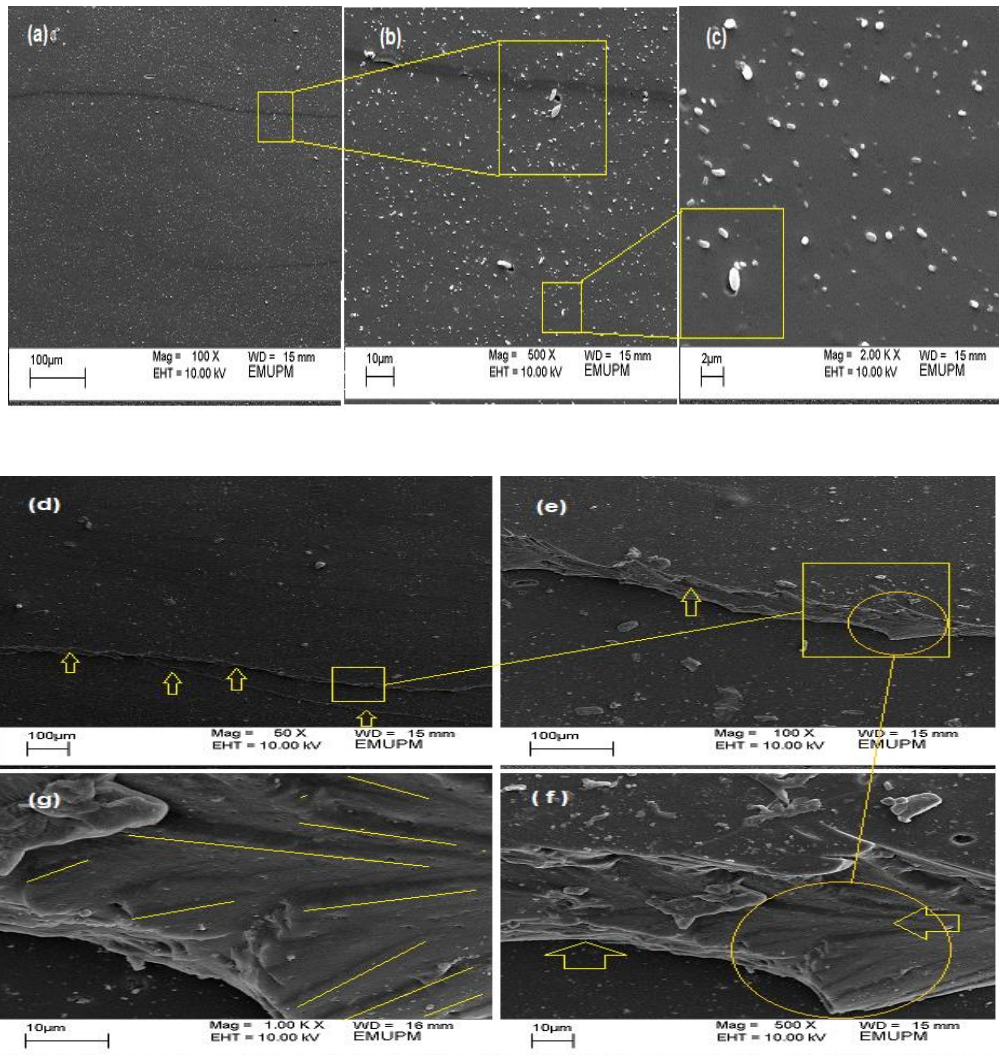


Fig. 9. Unfilled vulcanized NBR with ductile fracture at (a) Mag.=100x, flat fracture, (b) Mag.=500x – vulcanization additives (particles), (c) Mag.=2000x homogeneity. GNP/NBR rubber nanocomposite reinforced by 1.2 phr GNP at (d) Mag.=50x, lines-layers of nanocomposite, (e) Mag.=100x Plastic-elastic fracture (f) Mag.=500x – Flex-brittle fracture of sharp layers, (g) Mag.=1000x- lined curved fractures on the surface due to the tensile stress.

vulcanization additives. The unfilled NBR in Fig. (9-b) revealed a ductile fracture of smooth surface of the rubber matrix. The containing particles are the ZnO, they were distinguished clearly via (500x) magnification and spread out homogenously.

At (2000x) of the same sample, Fig. (9-c)

manifests that the pulled-out particles were in agglomeration feature with 1-2 μm diameters. They were found in very few locations of the NBR matrix; however the NBR rubber was tough with high elongation property. The cross-sectional analysis of 1.2 phr of GNP in GNP/NBR

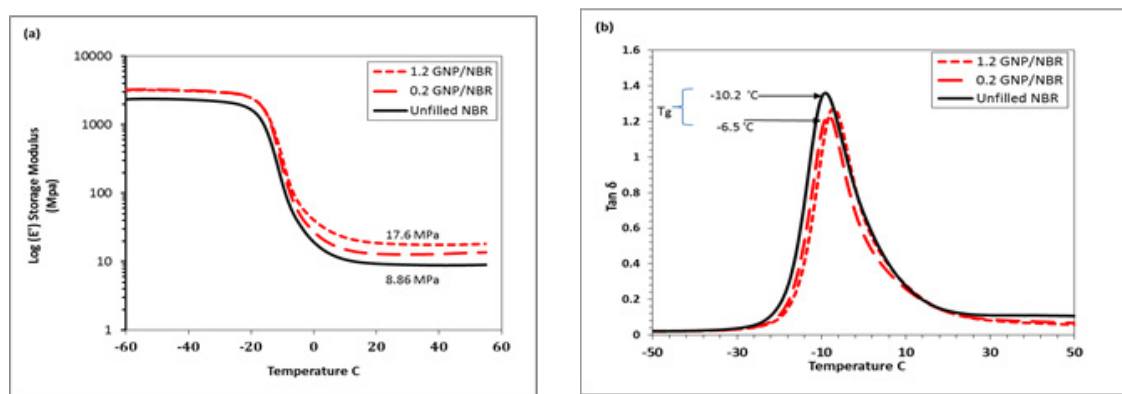


Fig. 10. DMA of unfilled NBR and GNP/NBR nanocomposite, (a) storage modulus as a function to the temperature, (b) $\tan \delta$ versus temperature.

nanocomposite was scanned to evaluate the dispersion level through the fracture type in Figs. (9-d) and (9-e).

There were flexible-brittle fractures observed with lines pattern at 50 and 100x. The brittleness is attributed to the influence of GNP by modifying the rubber structure from plastic phase to toughened elastic phase, as shown in Fig. (9-f) with 500x. Layers of rubber nanocomposites also appeared to have lines and wavy textures due to the tensile stress effect, as shown in the Fig. (9-g) at 1000x. This was compatible with the reported tests of the surface for verifying the strength of the interfacial linkage between graphene fillers and polymer matrix [29, 30]. GNP exhibited a homogenous dispersion due to combining two mixing techniques, which reflected on the affinity between the phases. At a content of 1.2 phr GNP, the dispersed particles seem to be fully encapsulated in the matrix with no obvious agglomerations or phase separation observed. The uniform dispersion of GNP in the NBR enhanced the stress transfer through the composites, which led to improve the properties of the GNP/NBR rubber nanocomposites.

Dynamic mechanical analysis

The dynamic mechanical characteristic was further studied to obtain the (GNP) effect upon the (GNP/NBR) nanocomposite storage modulus under a range of temperatures. Fig. (10-a) shows the changes in $\log E'$ of GNP/NBR nanocomposite with low and high contents 0.2 and 1.2 phr, respectively of GNP versus the temperature. E' measures the stiffness and stress bearing capability of the rubber nanocomposite. The improvement

in E' of GNP/NBR nanocomposite at 1.2 phr of GNP was larger than that of 0.2 phr of GNP and that of the unfilled NBR. It should be attributed to increases of the filler-filler interaction and density of the rubber nano composite. It is also explained by ($\tan \delta$) of the rubber nanocomposites via the range of temperature from (-30) to (15°C) as shown in the Fig. (10-b), which is called glass transition temperature (T_g). In this range, a major transition as the polymer goes from hard glassy to a rubbery state. Therefore, the T_g of NBR and the composites was calculated from the peak of the ($\tan \delta$ - temperature) curve in the figure above. In comparison with unfilled NBR, T_g of the GNP/NBR nanocomposites was obviously shifted a little toward to the high temperature because of the GNP contents of 0.2 and 1.2 phr in the composites. The physicochemical interaction between GNP and matrix of NBR matrix constrained the rubber molecular chains motion, which led to reduce the damping capability of NBR system.

CONCLUSIONS

The dispersion of GNP in Acrylo-NBR (dry rubber) using solution mixing method was performed successfully for preparing GNP/NBR rubber nanocomposite. The homogeneity of this composite was the most important target for improving its properties. It is achieved by adjusting GNP exfoliation in Tritonx-100/acetone in aqueous base by sonication and optimizing the compatibility between GNP suspension and NBR solution experimentally. The dispersion of GNP into NBR entirely was characterized by XRD and analyzed via the SEM of fractured surfaces morphology

of the composites samples. The nanocomposite crosslinking density was improved up to 42.3% at 1.2 phr of GNP. This is confirmed by the increase of the torques with less curing times due to the constraint of the rubber chains mobility. Also, the modulus of the GNP/NBR rubber nanocomposite at (M_{100}) increased three times more than the unfilled NBR and storage modulus to about 100% when T_g improved from (-10.2) to (-6.5°C), which is attributed to the good adhesion between GNP and NBR. At the same content 1.2% of GNP, there was enhancement in the hardness to about 13.2% as well.

CONFLICT OF INTEREST

The authors declare that there is no conflict of interests regarding the publication of this manuscript.

REFERENCES

- Li B, Zhong W-H. Review on polymer/graphite nanoplatelet nanocomposites. *Journal of Materials Science*. 2011;46(17):5595-614.
- Fim FdC, Guterres JM, Basso NRS, Galland GB. Polyethylene/graphite nanocomposites obtained by in situ polymerization. *Journal of Polymer Science Part A: Polymer Chemistry*. 2010;48(3):692-8.
- Kuila T, Bose S, Mishra AK, Khanra P, Kim NH, Lee JH. Chemical functionalization of graphene and its applications. *Progress in Materials Science*. 2012;57(7):1061-105.
- Yakovlev AV, Finaenov AI, Zabud'kov SL, Yakovleva EV. Thermally expanded graphite: Synthesis, properties, and prospects for use. *Russian Journal of Applied Chemistry*. 2006;79(11):1741-51.
- Yasmin A, Luo J-J, Daniel IM. Processing of expanded graphite reinforced polymer nanocomposites. *Composites Science and Technology*. 2006;66(9):1182-9.
- Geng Y, Wang SJ, Kim J-K. Preparation of graphite nanoplatelets and graphene sheets. *Journal of Colloid and Interface Science*. 2009;336(2):592-8.
- Kalaitzidou K, Fukushima H, Drzal LT. Multifunctional polypropylene composites produced by incorporation of exfoliated graphite nanoplatelets. *Carbon*. 2007;45(7):1446-52.
- Li Y, Wang Q, Wang T, Pan G. Preparation and tribological properties of graphene oxide/nitrile rubber nanocomposites. *Journal of Materials Science*. 2011;47(2):730-8.
- Nakazawa S, Okada K, Kunugi T. Wet Friction Characteristics of New Resilient Graphitic Friction Material. *Transactions of the Japan Society of Mechanical Engineers Series C*. 1994;60(572):1376-81.
- Mahmoud WE, Al-Ghamdi AA. Charge transport mechanism of graphite-nanosheet-loaded rubber nanocomposites. *Polymer International*. 2011;61(1):51-4.
- Wang LL, Zhang LQ, Tian M. Mechanical and tribological properties of acrylonitrile-butadiene rubber filled with graphite and carbon black. *Materials & Design*. 2012;39:450-7.
- Kim H, Miura Y, Macosko CW. Graphene/Polyurethane Nanocomposites for Improved Gas Barrier and Electrical Conductivity. *Chemistry of Materials*. 2010;22(11):3441-50.
- Zhan Y, Wu J, Xia H, Yan N, Fei G, Yuan G. Dispersion and Exfoliation of Graphene in Rubber by an Ultrasonically-Assisted Latex Mixing and In situ Reduction Process. *Macromolecular Materials and Engineering*. 2011;296(7):590-602.
- Yang J, Tian M, Jia Q-X, Shi J-H, Zhang L-Q, Lim S-H, et al. Improved mechanical and functional properties of elastomer/graphite nanocomposites prepared by latex compounding. *Acta Materialia*. 2007;55(18):6372-82.
- Galpaya D, Wang M, Liu M, Motta N, Waclawik E, Yan C. Recent Advances in Fabrication and Characterization of Graphene-Polymer Nanocomposites. *Graphene*. 2012;01(02):30-49.
- Varghese TV, Ajith Kumar H, Anitha S, Ratheesh S, Rajeev RS, Lakshmana Rao V. Reinforcement of acrylonitrile butadiene rubber using pristine few layer graphene and its hybrid fillers. *Carbon*. 2013;61:476-86.
- Ponnamma D, Maria HJ, Chandra AK, Thomas S. Rubber Nanocomposites: Latest Trends and Concepts. *Advanced Structured Materials: Springer Berlin Heidelberg*; 2013. p. 69-107.
- Samaržija-Jovanović S, Jovanović V, Marković G, Marinović-Cincović M. The effect of different types of carbon blacks on the rheological and thermal properties of acrylonitrile butadiene rubber. *Journal of Thermal Analysis and Calorimetry*. 2009;98(1):275-83.
- Zaleski R, Stefaniak W, Gorgol M, Gil M, Krasucka P, Goworek J. Swelling of cross-linked polymers in silicones of different molecular weight. *Polymer*. 2019;179:121611.
- Reza Saeb M, Sarami R, Iranpak B, Gaffari R. Tensile Properties of Natural Rubber Nanocomposites Affected by Crosslink Density. *Advances in Materials Physics and Chemistry*. 2012;02(04):260-3.
- Mensah B, Kim S, Arepalli S, Nah C. A study of graphene oxide-reinforced rubber nanocomposite. *Journal of Applied Polymer Science*. 2014;131(16):n/a-n/a.
- White JL. Rheological Behavior and Processing of Unvulcanized Rubber. *Science and Technology of Rubber: Elsevier*; 2005. p. 237-319.
- Leblanc J. Rubber-filler interactions and rheological properties in filled compounds. *Progress in Polymer Science*. 2002;27(4):627-87.
- Song SH, Jeong HK, Kang YG, Cho CT. Physical and thermal properties of acid-graphite/styrene-butadiene-rubber nanocomposites. *Korean Journal of Chemical Engineering*. 2010;27(4):1296-300.
- Barlow FW. Introduction to Compounding. *Rubber compounding: CRC Press*; 2018. p. 1-7.
- Murov S. Reaction-Map of Organic Chemistry. *Journal of Chemical Education*. 2007;84(7):1224.
- Li ZH, Zhang J, Chen SJ. Effects of carbon blacks with various structures on vulcanization and reinforcement of filled ethylene-propylene-diene rubber. *Express Polymer Letters*. 2008;2(10):695-704.
- Zaeimoedin TZ, Mustafa Kamal M, Che Aziz AK. Rheological Properties and Extrusion Performance Evaluation of Silica Filled Epoxidized Natural Rubber (ENR) Compounds as Compared to Natural Rubber/ Butadiene Rubber (NR/BR) Compound. *Advanced Materials Research*. 2016;1133:236-240.
- Das A, Kasaliwal GR, Jurk R, Boldt R, Fischer D, Stöckelhuber

- KW, et al. Rubber composites based on graphene nanoplatelets, expanded graphite, carbon nanotubes and their combination: A comparative study. *Composites Science and Technology*. 2012;72(16):1961-7.
30. Ramanathan T, Abdala AA, Stankovich S, Dikin DA, Herrera-Alonso M, Piner RD, et al. Functionalized graphene sheets for polymer nanocomposites. *Nature Nanotechnology*. 2008;3(6):327-31.
31. Mousa A, Heinrich G, Simon F, Wagenknecht U, Stöckelhuber K-W, Dweiri R. Carboxylated nitrile butadiene rubber/hybrid filler composites. *Materials Research*. 2012;15(4):671-8.
32. Mousa A, Heinrich G, Wagenknecht U. Cure Characteristics and Mechanical Properties of Carboxylated Nitrile Butadiene Rubber (XNBR) Vulcanizate Reinforced by Organic Filler. *Polymer-Plastics Technology and Engineering*. 2011;50(13):1388-92.
33. Wu Y-P, Wang Y-Q, Zhang H-F, Wang Y-Z, Yu D-S, Zhang L-Q, et al. Rubber–pristine clay nanocomposites prepared by co-coagulating rubber latex and clay aqueous suspension. *Composites Science and Technology*. 2005;65(7-8):1195-202.
34. Hernández M, Bernal MdM, Verdejo R, Ezquerro TA, López-Manchado MA. Overall performance of natural rubber/graphene nanocomposites. *Composites Science and Technology*. 2012;73:40-6.
35. Chandrasekaran S, Seidel C, Schulte K. Preparation and characterization of graphite nano-platelet (GNP)/epoxy nano-composite: Mechanical, electrical and thermal properties. *European Polymer Journal*. 2013;49(12):3878-88.
36. Bhowmick AK, Bhattacharya M, Mitra S, Kumar KD, Maji PK, Choudhury A, et al. Morphology–Property Relationship in Rubber-Based Nanocomposites: Some Recent Developments. *Advanced Rubber Composites*: Springer Berlin Heidelberg; 2010. p. 1-83.
37. Bai X, Wan C, Zhang Y, Zhai Y. Reinforcement of hydrogenated carboxylated nitrile–butadiene rubber with exfoliated graphene oxide. *Carbon*. 2011;49(5):1608-13.
38. Ismail MN, Khalaf AI. Styrene-butadiene rubber/graphite powder composites: Rheometrical, physicomechanical, and morphological properties. *Journal of Applied Polymer Science*. 2010;120(1):298-304.
39. Yang J, Tian M, Jia Q-X, Zhang L-Q, Li X-L. Influence of graphite particle size and shape on the properties of NBR. *Journal of Applied Polymer Science*. 2006;102(4):4007-15.
40. Sadasivuni KK, Ponnamma D, Thomas S, Grohens Y. Evolution from graphite to graphene elastomer composites. *Progress in Polymer Science*. 2014;39(4):749-80.
41. Singh V, Joung D, Zhai L, Das S, Khondaker SI, Seal S. Graphene based materials: Past, present and future. *Progress in Materials Science*. 2011;56(8):1178-271.
42. Yang J, Zhang L-Q, Shi J-H, Quan Y-N, Wang L-L, Tian M. Mechanical and functional properties of composites based on graphite and carboxylated acrylonitrile butadiene rubber. *Journal of Applied Polymer Science*. 2010:NA-NA.
43. Zhao X, Zhang Q, Chen D, Lu P. Enhanced Mechanical Properties of Graphene-Based Poly(vinyl alcohol) Composites. *Macromolecules*. 2010;43(5):2357-63.
44. Blanton TN, Majumdar D, Melpolder SM. Microstructure and Physical Properties of Clay-Polymer Composites. *MRS Proceedings*. 2000;628.